Application value of iterative reconstruction with CTA to intractable headache patients

YANFENG XU, SHUJING YU, LI ZHANG, JING ZHENG, YUEFENG CHEN and YANXU CHE

Department of CT Diagnosis, Cangzhou Central Hospital, Cangzhou, Hebei 061001, P.R. China

Received September 14, 2017; Accepted April 17, 2018

DOI: 10.3892/etm.2018.6232

Abstract. Application value of iterative reconstruction with computed tomographic angiography (CTA) in the patients with intractable headache was investigated. One hundred and eighty patients with headache, who were admitted and treated in Cangzhou Central Hospital, were selected to undergo CTA scan. The patients were divided into group A, B and C according to different scanning conditions and data reconstruction techniques. In group A, the scanning parameters were 120 kV and 300 mA, and filtered back projection (FBP) algorithm was used for data reconstruction. In group B, the scan parameters were 100 kV and automatic milliamperes. Further, adaptive iterative dose reduction via three-dimensional processing (AIDR-3D) was used for data reconstruction. In group C, the scan parameters were 80 kV with automatic milliamperes, and AIDR-3D technique was utilized for data reconstruction. The CT value, noise, signal-to-noise ratio (SNR), contrast-to-noise ratio (CNR), subjective assessment score of image quality and radiation dose of the three groups of images were compared. There were significant differences in CT values, standard deviation (SD) values, SNRs and CNRs of different vessel segments and muscles among the three groups ($P<0.05$). The image assessment scores at the levels of the atlas and C7 vertebra as well as those of the brain parenchyma in the three groups had notable differences ($P<0.05$). However, they showed no differences at the level of the C4 vertebra ($P>0.05$). Further, significant differences were observed in volume computed tomography dose index ($CTDI_{vol}$), dose-length product (DLP) and effective dose (ED) ($P<0.05$). In conclusion, for patients with intractable headache, the image quality of the CTA scan using AIDR-3D reconstruction method showed better results over FBP reconstruction method. Further, best results were observed when the scan parameters were 100 kV, automatic milliamperes and the data reconstruction was performed by AIDR-3D.

Correspondence to: Dr Shujing Yu, Department of CT Diagnosis, Cangzhou Central Hospital, 16 Xinhuaxi Road, Yunhe, Cangzhou, Hebei 061001, P.R. China
E-mail: czct2075570@163.com

Key words: iterative reconstruction, CT examination, intractable headache

Introduction

Intractable headache is a common neurological disease in clinical practice, which has the traits of insidious onset, prolonged symptoms, lingering and recurrent course. Generally, migraine, trigeminal autonomic cephalgia and recurrent headache of tension headache belong to the intractable headache (1). Patients with intractable headache often have paroxysmal pain of moderate to severe levels, accompanied by nausea, dizziness, vomiting and blurred vision. Limb weakness, triggered stroke, angina pectoris, affective disorders and other typical features were also observed to be associated. Moreover, intractable headache has serious impact on the patients' social function and quality of life similar to chronic diseases like severe mental diseases, quadriplegia and dementia (2).

Computed tomographic angiography (CTA) has the advantages of high spatial resolution and high-density resolution. Also, it is non-invasive in nature therefore, it is widely favored by doctors and patients in clinic. Furthermore, it is used as the major means of diagnosis for coronary artery diseases, especially stable angina (3,4). The clinical diagnosis of intractable headache is mainly based on the complaints told by patients. The CTA examinations are often needed for confirmation in order to identify the cause of disease. However, few studies on the application of CTA to the diagnosis of intractable headache exist in the literature. In the present study, CTA examinations combined with different reconstruction techniques were conducted for the patients with intractable headache, and their characteristics were analyzed.

Materials and methods

General information. One hundred and eighty patients with intractable headache, who were admitted and treated in Cangzhou Central Hospital (Cangzhou, China) from June 2016 to May 2017, were enrolled. Inclusion criteria: i) Patients who received CTA examinations; and ii) patients who signed the informed consent. Exclusion criteria: i) Patients complicated with other severe chronic diseases; and ii) patients complicated with psychiatric disorders that could not coordinate with the examinations. The patients were divided into three groups, namely, group A (n=60), group B (n=60) and group C (n=60), by means of random number table. In group A, the scan parameters were 120 kV and 300 mA, and filtered back projection (FBP) algorithm was used for data reconstruction; in group B, the scan parameters were 100 kV and automatic milliamperes, and adaptive iterative dose reduction using three-dimensional processing

Table I. Comparison of baseline data among three groups of patients.

Item	Group A (n=60)	Group B (n=60)	Group C (n=60)	P-value
Sex (male/female)	28/32	27/33	33/27	0.502
Age (years)	25-78	30-80	33-80	
Average age (years)	58.36±9.49	60.25±9.51	58.37±9.46	0.471
BMI (kg/m^2)	23.38±3.54	24.47±3.53	24.51±4.23	0.162
Educational level (n, %)				
Junior high school and below	9 (15.00)	7 (11.67)	8 (13.33)	0.374
Senior high school and special secondary school	28 (46.67)	27 (45.00)	30 (50.00)	
College and above	23 (38.33)	26 (43.33)	22 (36.67)	

BMI, body mass index.

Table II. Comparison of CT values of different muscles among the three groups of patients (Hu).

Group	Cases	Right masticatory muscle	Right sternocleidomastoid	Lower sternocleidomastoid	Average value of muscle
Group A	60	61.82±7.43	60.13±7.47	61.26±9.18	61.09±5.12
Group B	60	63.24±9.26	63.05±6.96	62.93±14.15	63.06±6.85
Group C	60	66.17±10.73	63.57±9.32	71.28±16.74	67.97±7.74
F-value		11.573	2.132	21.658	10.352
P-value		<0.001	0.048	<0.001	<0.001

Table III. Comparison of CT values of different vessel segments among the three groups of patients (Hu).

Group	Cases	Right internal carotid artery	Right carotid sinus	Common carotid artery	Average value of blood vessel
Group A	60	392.65±52.61	394.62±50.67	358.56±53.38	381.89±50.72
Group B	60	502.93±78.46	515.13±79.86	467.87±79.07	495.74±77.26
Group C	60	683.32±142.83	686.65±149.53	625.46±136.64	665.17±139.14
F-value		56.348	67.821	63.258	64.714
P-value		<0.001	<0.001	<0.001	<0.001

(AIDR-3D) was used for data reconstruction; in group C, the scan parameters were 80 kV and automatic milliamperes, and AIDR-3D technique was utilized for data reconstruction. There was no statistically significant difference in the general information among the three groups (P>0.05) (Table I). The Ethics Committee of Cangzhou Central Hospital approved the study. All patients provided written informed consents.

Methods

Preparations before examinations. Before the examinations, all the patients fasted for more than 4 h; the medical staff presented the cautions of the examinations, provided psychological comfort for the patents so as to eliminate their negative emotions, and informed the patients of removing all the metal objects on them.

CTA examinations. The patients were examined by the Toshiba Aquilion™ ONE 320-row helical CT machine (Toshiba Corp., Tokyo, Japan). The parameters of group A were set as 120 kV and 300 mA, group B as 100 kV and automatic milliamperes, and group C as 80 kV and automatic milliamperes. Iopamidol injection (Iopamidol) (Patheon Italia S.p.A., Ferentino, Italy; sub-packaging: BRACCO; approval no. NMPN J20150090) was used as the contrast agent. The concentration used was 370 mg iodine/ml, 25 ml of 0.9% sodium chloride was injected with an injection rate of 5 ml/sec. Scanning mode: Helical acquisition. The patient was guided to stay in the supine position with both hands naturally falling on both sides of the body; then the CT scan was performed for the patient's neck and head, from the level of the aortic arch to the level of the top of the head.

Image reconstruction. In group A, FBP was used for CT image reconstruction; in group B and group C, AIDR-3D was utilized for reconstruction, followed by transmission and import of scan data into the Vitrea Workstation provided by Toshiba Corp. for processing.

Table IV. Comparison of SD values of different vessel segments among the three groups of patients (Hu).

Groups	Case	Right internal carotid artery	Right carotid sinus	Common carotid artery	Average value of blood vessel
Group A	60	14.78±3.58	10.43±3.15	25.96±3.79	16.67±3.42
Group B	60	17.94±3.62	14.48±3.26	15.26±3.34	15.34±3.06
Group C	60	19.58±3.85	17.58±3.47	19.69±3.53	18.67±3.64
F-value		11.628	14.578	26.942	7.275
P-value	<0.001	<0.001	<0.001	<0.001	

SD, standard deviation.

Table V. Comparison of SD values of different muscles among the three groups of patients (Hu).

Groups	Case	Right masticatory muscle	Right sternocleidomastoid	Lower sternocleidomastoid	Average value of muscle
Group A	60	12.96±2.13	8.18±2.14	14.19±3.16	11.32±2.32
Group B	60	14.76±3.06	11.34±1.97	12.96±2.15	12.34±2.45
Group C	60	17.73±10.73	14.42±2.78	16.16±3.14	15.67±3.56
F-value		3.152	2.147	5.769	6.489
P-value		0.026	0.037	<0.001	<0.001

SD, standard deviation.

Evaluation indexes. The noise [standard deviation (SD)] values and CT values of the blood vessels (right internal carotid artery, right carotid sinus and common carotid artery) and muscles (right masticatory muscle, right sternocleidomastoid and lower sternocleidomastoid) under different reconstruction algorithms were measured. The signal-to-noise ratio (SNR) and contrast-to-noise ratio (CNR) were then calculated. Formula: SNR = CT value/SD value, CNR = (average CT value of blood vessel - average CT value of muscle)/SD value (5).

The volume-computed tomography dose index ($CTDI_{vol}$) and scan length (L) of each group were recorded. Further, the dose-length product (DLP) and effective dose (ED) were calculated according to the formula. Relevant formula: DLP = $CTDI_{vol}$ x L; ED = DLP x k, of which k = 0.0031 (6).

The CT images of different reconstruction techniques were reviewed and graded by two senior imaging technicians (with a work experience of more than 10 years) using double-blind method and 5-point scoring system, respectively. Criteria: Excellent images with good clarity, and the contrast were give maximum 5-points and were assigned as ***e***. Images with reiable contrast and clarity were given 4-points and were assigned as ***d***. Images with with mild artifacts, were given 3-points and were graded as ***c***; further, poor images blurring, and staggered layers were given 2-points and were graded as ***b***. Extremely poor images with serious artifacts were given only 1-point and were graded as ***a***. Furthermore, for presentation of results, scores were presented as the average scores of all patients in each group.

Statistical analysis. Statistical Product and Service Solutions (SPSS) 19.0 (IBM Corp., Armonk, NY, USA) software was utilized for data processing. The measurement data are presented as mean ± standard deviation. Further analysis of variance was applied for intragroup data and the post hoc test was Least Significant Difference test. P<0.05 was considered to indicate a statistically significant difference.

Results

Comparison of CT values among the three groups of patients. The average CT values of different muscles were significantly higher in group C (61.09±5.12), followed by group B (63.06±6.85) and were least in group A (61.09±5.12) (P<0.001) (Table II). Similar trend was observed in the average CT values of vessel segments (P<0.001) (Table III).

Comparison of SD values among the three groups of patients. There were remarkable differences in SD values of different vessel segments and muscles among the three groups. The average SD values were least in group A (16.67±3.42) followed by group B (15.34±3.06) and were highest in group C (18.67±3.64) (P<0.001) (Table IV). Similar trend was noticed in the average SD values of vessels in all 3 groups (P<0.001) (Table V).

Comparisons of SNRs among the three groups of patients. There were notable differences in SNRs of different vessel segments among the three groups. The highest average SNR value was in group C (18.67±3.64). Further, the least average SNR values was noted in group A (27.67±3.23) and the value of group B (33.46±3.46) was significantly higher (P<0.001) but was comparatively lower in comparison with group C (P<0.001) (Table VI).

Comparison of CNRs among the three groups of patients. The CNRs followed similar trend to those noted in other

Table VI. Comparison of SNRs of different vessel segments among the three groups of patients.

Group	Case	Right internal carotid artery	Right carotid sinus	Common carotid artery	Average value of blood vessel
Group A	60	30.25±3.27	36.49±3.35	17.65±3.16	27.67±3.23
Group B	60	32.64±3.54	38.68±3.67	33.26±3.48	33.46±3.46
Group C	60	39.23±3.76	42.02±3.87	35.19±3.57	38.58±3.65
F-value		11.572	12.926	27.825	21.354
P-value		<0.001	<0.001	<0.001	<0.001

SNRs, signal-to-noise ratios.

Table VII. Comparison of CNRs of different vessel segments among the three groups of patients.

Group	Case	Internal carotid artery	Carotid sinus	Right common carotid artery	Average value of blood vessel
Group A	60	24.98±3.13	33.21±3.48	17.98±3.04	22.37±3.12
Group B	60	28.56±3.35	36.41±3.56	29.94±3.25	29.18±3.14
Group C	60	34.13±3.56	39.29±3.39	32.93±3.43	34.26±3.58
F-value		21.925	19.783	29.472	26.538
P-value		<0.001	<0.001	<0.001	<0.001

CNRs, contrast-to-noise ratio.

Table VIII. Comparison of assessment scores of image quality among the three groups of patients.

Group	Case	Level of the atlas	Level of the C7 vertebra	Level of the C4 vertebra	Brain parenchyma
Group A	60	4.68±0.39	3.17±0.98	4.93±0.27	4.75±0.37
Group B	60	4.80±0.36	4.51±0.50	4.98±0.09	4.44±0.50
Group C	60	4.61±0.38	4.11±0.57	4.93±0.19	4.52±0.59
F-value		6.364	7.923	0.087	3.528
P-value		<0.001	<0.001	0.136	<0.001

Scores are presented as the average scores of all patients in each group.

indices. This included highest average CNR value in group C (22.37±3.12) followed by group B (22.37±3.12) and least average CNR value in group A (22.37±3.12). All differences were statically significant (P<0.001) (Table VII).

Comparison of assessment scores of image quality among the three groups of patients. The image assessment scores at the levels of the atlas and C7 vertebra as well as those of the brain parenchyma among the three groups had notable differences (P<0.05) but had no obvious differences at the level of the C4 vertebra (P>0.05) (Table VIII; Fig. 1). The scores were the average scores of all patients in each group. Fig. 1B appeared best in quality as it belonged to group B that revealed significantly the highest average scores at all three levels viz. atlas, c7 vertebra and brain parenchyma (Table VIII). It also appeared good at the level of C4 vertebra but the differences were not statistically significant at this level among the three groups.

Comparison of radiation doses among the three groups. The $CTDI_{vol}$ was observed to be highest in group A. Further statistical significant decline was noted in the $CTDI_{vol}$ of group B (P<0.01). Similar significant decrease was also recorded in group C. DLP and ED values revealed similar trend with statistical significant decrease in groups B and C when compared with group A (P<0.001) (Table IX).

Discussion

The incidence rate of primary headache among the people aged 18-65 years is 23.8%, according to the Chinese epidemiologic investigation in 2010. Currently, the World Health Organization (WHO) has classified headache as one of the ten medical conditions that are disabling (7). There are multiple factors responsible for intractable headache, such as dietary factors, emotional factors, smoking and drinking, sleeping habits, pressure changes, muscular tension, inflammation (sinusitis),

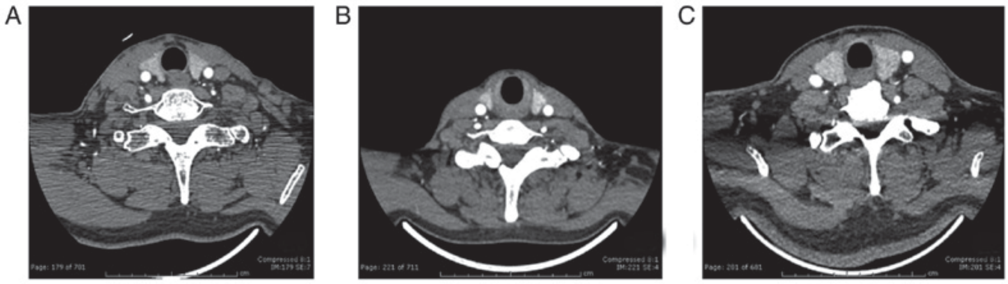

Figure 1. (A) Male, 66 years, paroxysmal severe headache, paroxysmal dizziness accompanied by blurred vision; image after reconstruction with 120 kV, 300 mA and FBP; (B) male, 60 years, paroxysmal moderate headache, intermittent dizziness; image after reconstruction with 100 kV, automatic milliamperes and AIDR-3D; (C) female, 58 years, moderate headache, paroxysmal dizziness; image after reconstruction with 80 kV, automatic milliamperes and AIDR-3D.

Table IX. Comparison of radiation doses among the three groups.

Group	Case	$CTDI_{vol}$ (mGy)	DLP (mGy.cm)	ED (msv)
Group A	60	14.71±2.13	580.36±26.34	1.80±0.08
Group B	60	4.36±1.14	169.75±46.82	0.53±0.15
Group C	60	3.67±0.62	141.06±25.37	0.44±0.08
F-value		17.836	56.394	11.627
P-value		<0.001	<0.001	<0.001

$CTDI_{vol}$, computed tomography dose index; DLP, dose-length product; ED, effective dose.

cervical spondylosis and endocrine factors. Patients with intractable headache not only have vegetative nerve symptoms, but also manifested as phonophobia and photophobia. They are often complicated with changes in psychology and personality. This included lack of strength, laziness in talking, irritability, frigidity and other symptoms (8). Till now there is no effective method for treatment of intractable headache, and symptomatic therapies are often utilized.

CT utilization begun in clinical practices in the 1970s, as it offered features that were irreplaceable by other radiological examinations (9). For patients with intractable headache, the noninvasive operation of the CTA scan is quite acceptable. So, it played a crucial role in the diagnosis and treatment. However, the radiation hazards caused by the CTA scan still cannot be avoided. Therefore, search for the possible ways to reduce the radiation dose without affecting image quality still remains the research hotspot in the clinical studies (10).

With the advent and application of CT, FBP is used as the major CT image reconstruction technique. The reconstructed images can be obtained quickly through FBP by virtue of calibration, weighting, filtering and back projection of the projection values as well as simple algorithm building systems. However, the image quality shows decline with the reduced radiation dose (11,12). In recent years, the major CT manufacturers are continuously improving the reconstruction techniques, and many iterative reconstruction algorithms have been widely applied in clinical practices. For example, General Electric (GE) Co. released the adaptive statistical iterative reconstruction (ASIR) in 2008 and model-based iterative reconstruction (MBIR) in 2009; in 2010, and Siemens introduced the raw-data based iterative reconstruction-SAFIRE (Sinogram Affirmed Iterative Reconstruction); Toshiba Corp. launched the AIDR in 2010 (13). All these techniques make estimated synthetic projections on the images, then the differences between the estimated projections and the actual objects were compared. Finally the reconstructed images were formed after calibration by multiple times of iterative procedures (14). In the present study, the results showed that the differences in the CT values of different vessel segments and muscles among the three groups were significant, of which the CT values in group B and C were significantly higher than those in group A (P<0.05). The above observation could be due to the differences in the parameters of tube voltage during scanning of the three groups. The tube voltage could affect the wavelength of radiation, thus influencing the penetration ability of X-ray, leading to a change in attenuation coefficient of the X-ray. Therefore, the CT value showed a gradual increase with decreasing tube voltage (15).

The present study results indicated that there were significant differences in SD values, SNRs and CNRs among the three groups (P<0.05). The image assessment scores at the levels of the atlas and C7 vertebra as well as those of the brain parenchyma among the three groups had notable differences (P<0.05) but had no obvious differences at the level of the C4 vertebra (P>0.05). The overall image quality in group B and C were remarkably better than that in group A, and group B had the best image quality. The Toshiba Aquilion™ ONE 320-row helical CT machine utilizes a large-area quantum detector, so that the scan data could be acquired by merely rotating the rack a circle without moving the bed. As a result, the artifacts caused by previous helical motions were reduced. However, FBP has relatively high requirements for the raw data; in particular, it is vulnerable to the quantities of photons needed for projection imaging, of which SD, SNR and CNR are more vulnerable; therefore, it is possible that the image quality cannot meet the diagnostic demand (16,17). Reconstruction with AIDR-3D is less affected by image noises; after several iterative procedures and constant optimization of noises, the SNR and CNR could be increased, so as to meet the diagnostic demands by guaranteeing the image quality (18).

In clinical practices, the applied radiation dose could be influenced by means of optimizing tube current and tube voltage, thus lowering the production of radiation dose in varying degrees (19). In the present study, the results revealed that there were significant differences in $CTDI_{vol}$, DLP and ED among the three groups, of which the values in group B and C were significantly lower than those in group A ($P<0.05$). It could be justified by the fact that, the X-radiation received during the examinations was reduced as tube voltages in group A, B and C were decreased constantly. Also, the absorbed dose and ED of the tested blood vessels and muscles in the patients showed decrease in variable degrees. The utilization of iterative reconstruction technique could elevate the detection efficiency of iodine signals, and the examination results would not be affected even though the tube voltage was appropriately lowered, thus providing some space for decreasing $CTDI_{vol}$, DLP and ED (20).

In conclusion, compared with reconstruction with FBP, reconstruction with AIDR could decrease the radiation dose in the CTA examinations on patients with intractable headache. It also helps in reduction of radiation hazards to the patients and improves the image quality.

Acknowledgements

Not applicable.

Funding

No funding was received.

Availability of data and materials

The datasets used and/or analyzed during the current study are available from the corresponding author on reasonable request.

Authors' contributions

YX wrote the manuscipt. YX and SY were repsonsible for CTA examinations. LZ and JZ collected and analyzed the general data of patients. YuC and YaC recorded and interpreted evaluation indexesAll authors read and approved the final manuscript.

Ethics approval and consent to participate

The Ethics Committee of Cangzhou Central Hospital (Cangzhou, China) approved the study. All patients provided written informed consents.

Patient consent for publication

Not applicable.

Competing interests

The authors declare that they have no competing interests.

References

1. Hawro T, Bogucki A, Krupińska-Kun M, Maurer M and Woźniacka A: Intractable headaches, ischemic stroke, and seizures are linked to the presence of anti-β2GPI antibodies in patients with systemic lupus erythematosus. PLoS One 10: e0119911, 2015.
2. Kinfe TM, Schuss P and Vatter H: Occipital nerve block prior to occipital nerve stimulation for refractory chronic migraine and chronic cluster headache: Myth or prediction? Cephalalgia 35: 359-362, 2015.
3. Beeres M, Wichmann JL, Frellesen C, Bucher AM, Albrecht M, Scholtz JE, Nour-Eldin NE, Gruber-Rouh T, Lee C, Vogl TJ, *et al*: ECG-gated versus non-ECG-gated high-pitch dual-source CT for whole body CT angiography (CTA). Acad Radiol 23: 163-167, 2016.
4. Wilkinson EP, Shahidi R, Wang B, Martin DP, Adler JR Jr and Steinberg GK: Remote-rendered 3D CT angiography (3DCTA) as an intraoperative aid in cerebrovascular neurosurgery. Comput Aided Surg 4: 256-263, 1999.
5. Wachowicz K, Dezanche N, Yip E, Volotovskyy V and Fallone B: TU-H-BRA-09: Relationship between B0 and the contrast-to-noise ratio (CNR) of tumour to background for MRI/radiotherapy hybrids. Med Phys 43: 3770, 2016.
6. Atkins S: The relationship of CT mean modulated dose-length product and body mass index during routine 18F-FDG PET/CT studies. Int J Med Imaging 3: 94-97, 2015.
7. Rozen TD: Clomiphene citrate as a preventive treatment for intractable chronic cluster headache: A second reported case with long-term follow-up. Headache 55: 571-574, 2015.
8. Mitsikostas DD, Edvinsson L, Jensen RH, Katsarava Z, Lampl C, Negro A, Osipova V, Paemeleire K, Siva A, Valade D, *et al*: Refractory chronic cluster headache: A consensus statement on clinical definition from the European Headache Federation. J Headache Pain 15: 79, 2014.
9. Moser JB, Sheard SL, Edyvean S and Vlahos I: Radiation dose-reduction strategies in thoracic CT. Clin Radiol 72: 407-420, 2017.
10. Shih MC and Hagspiel KD: CTA and MRA in mesenteric ischemia: Part 1, Role in diagnosis and differential diagnosis. AJR Am J Roentgenol 188: 452-461, 2007.
11. Bahn YE, Kim SH, Kim MJ, Kim CS, Kim YH and Cho SH: Detection of urothelial carcinoma: Comparison of reduced-dose iterative reconstruction with standard-dose filtered back projection. Radiology 279: 471-480, 2016.
12. Padole A, Singh S, Lira D, Blake MA, Pourjabbar S, Khawaja RD, Choy G, Saini S, Do S and Kalra MK: Assessment of filtered back projection, adaptive statistical, and model-based iterative reconstruction for reduced dose abdominal computed tomography. J Comput Assist Tomogr 39: 462-467, 2015.
13. Zhao P, Hou Y, Liu Q, Ma Y and Guo Q: Radiation dose reduction in cardiovascular CT angiography with iterative reconstruction (AIDR 3D) in a swine model: A model of paediatric cardiac imaging. Clin Radiol 71: 716.e7-716.e14, 2016.
14. Nagatani Y, Takahashi M, Murata K, Ikeda M, Yamashiro T, Miyara T, Koyama H, Koyama M, Sato Y, Moriya H, *et al*; investigators of ACTIve study group: Lung nodule detection performance in five observers on computed tomography (CT) with adaptive iterative dose reduction using three-dimensional processing (AIDR 3D) in a Japanese multicenter study: Comparison between ultra-low-dose CT and low-dose CT by receiver-operating characteristic analysis. Eur J Radiol 84: 1401-1412, 2015.
15. Pan YN, Li AJ, Chen ZQ, Ren DW, Zhang J, Jiang MQ and Huang QL: Improved image quality and decreased radiation dose of lower extremity computed tomography angiography using low-tube-voltage and adaptive iterative reconstruction. J Comput Assist Tomogr 40: 272-276, 2016.
16. Blobel J, Mews J, Goatman KA, Schuijf JD and Overlaet W: Calibration of coronary calcium scores determined using iterative image reconstruction (AIDR 3D) at 120, 100, and 80 kVp. Med Phys 43: 1921-1932, 2016.
17. Mirsadraee S, Weir NW, Connolly S, Murchison JT, Reid JH, Hirani N, Connell M and van Beek EJ: Feasibility of radiation dose reduction using AIDR-3D in dynamic pulmonary CT perfusion. Clin Radiol 70: 844-851, 2015.
18. Dyakov I, Stoinova V, Groudeva V and Vassileva J: The influence of novel CT reconstruction technique and ECG-gated technique on image quality and patient dose of cardiac computed tomography. Radiat Prot Dosimetry 165: 182-184, 2015.
19. Kulkarni K, Lohit S, Turaga P, Kerviche R and Ashok A: ReconNet: Non-iterative reconstruction of images from compressively sensed measurements. In: Conference: 2016 IEEE Conference on Computer Vision and Pattern Recognition (CVPR), Seattle, WA, USA, pp449-458, 2016.
20. Schaafs LA, Lenk J, Hamm B and Niehues SM: Reducing the dose of CT of the paranasal sinuses: Potential of an iterative reconstruction algorithm. Dentomaxillofac Radiol 45: 20160127, 2016.